(Preprint) AAS 12-632

REALIZATION OF STATE-SPACE MODELS FOR WAVE PROPAGATION SIMULATIONS

Stephen A. Ketcham,[*] Minh Q. Phan,[†] Richard S. Darling, [‡] and Mihan H. McKenna[§]

Fully three-dimensional numerical solutions can quantify exterior seismic or acoustic propagation throughout complex geologic or atmospheric domains. Results from impulsive sources typically reveal propagating waves plus reverberations typical of multi-path scattering and wave-guide behavior, with decay toward quiescent motions as the dominant wave energy moves out of the domain. Because such computations are expensive and yield large data sets, it is advantageous to make the data reusable and reducible for both direct and reciprocal simulations. Our objective is efficient time-domain simulation of the wave-field response to sources with arbitrary time series. For this purpose we developed a practical and robust technique for superstable model identification. A superstable model has the form of a state-space model, but the output matrix contains the system dynamics. It simulates propagation with the fidelity of the pulse response calculated for the numerical system. Our development of the superstable technique was motivated by our initial application of the Eigensystem Realization Algorithm to wave-field systems from high-performance-computing analyses, where we recognized exterior propagation features allowing superstable model assignment. Most importantly the pulse response and its decay over the domain are captured in a finite duration, and decay to zero beyond a finite number of time steps implies a system with zero eigenvalues. We demonstrate propagation-system identification with pulse response data derived from supercomputer analysis, and conclude that, using superstable-identified systems, we are able to create reusable and reducible propagation-system models that accurately simulate the wave field using a fraction of the original computational resources.

INTRODUCTION

Simulating the propagation of seismic and acoustic energy involves solutions of wave equations. Fully three-dimensional numerical solutions can quantify propagation throughout complex geologic or atmospheric domains, and are sometimes necessary to support a physical understanding of practical scenarios without compromising realism. For example, sound or vibration propa-

[*] Research Physical Scientist, Cold Regions Research and Engineering Laboratory, U.S. Army Engineer Research and Development Center, 72 Lyme Rd., Hanover, NH 03755.
[†] Associate Professor, Thayer School of Engineering, Dartmouth College, 14 Engineering Drive, Hanover, NH 03755.
[‡‡] Research Mechanical Engineer, Signature Physics Branch, Cold Regions Research and Engineering Laboratory, U.S. Army Engineer Research and Development Center, 72 Lyme Rd., Hanover, NH 03755.
[§§] Research Geophysicist, Geotechnical and Structures Laboratory, U.S. Army Engineer Research and Development Center, 3909 Halls Ferry Road, Vicksburg, MS 39180.

Report Documentation Page

Form Approved
OMB No. 0704-0188

1. REPORT DATE	2. REPORT TYPE	3. DATES COVERED
2012		

4. TITLE AND SUBTITLE	5a. CONTRACT NUMBER
Realization Of State-Space Models For Wave Propagation Simulations	5b. GRANT NUMBER
	5c. PROGRAM ELEMENT NUMBER
6. AUTHOR(S)	5d. PROJECT NUMBER
	5e. TASK NUMBER
	5f. WORK UNIT NUMBER
7. PERFORMING ORGANIZATION NAME(S) AND ADDRESS(ES) **Cold Regions Research and Engineering Laboratory,U.S. Army Engineer Research and Development Center,Research Physical Scientist,Hanover,NH,03755**	8. PERFORMING ORGANIZATION REPORT NUMBER
9. SPONSORING/MONITORING AGENCY NAME(S) AND ADDRESS(ES)	10. SPONSOR/MONITOR'S ACRONYM(S)
	11. SPONSOR/MONITOR'S REPORT NUMBER(S)

12. DISTRIBUTION/AVAILABILITY STATEMENT
Approved for public release; distribution unlimited.

13. SUPPLEMENTARY NOTES
The original document contains color images.

14. ABSTRACT
Fully three-dimensional numerical solutions can quantify exterior seismic or acoustic propagation throughout complex geologic or atmospheric domains. Results from impulsive sources typically reveal propagating waves plus reverberations typical of multi-path scattering and wave-guide behavior, with decay toward quiescent motions as the dominant wave energy moves out of the domain. Because such computations are expensive and yield large data sets, it is advantageous to make the data reusable and reducible for both direct and reciprocal simulations. Our objective is efficient time-domain simulation of the wave-field response to sources with arbitrary time series. For this purpose we developed a practical and robust technique for superstable model identification. A superstable model has the form of a state-space model, but the output matrix contains the system dynamics. It simulates propagation with the fidelity of the pulse response calculated for the numerical system. Our development of the superstable technique was motivated by our initial application of the Eigensystem Realization Algorithm to wave-field systems from high-performance-computing analyses where we recognized exterior propagation features allowing superstable model assignment. Most importantly the pulse response and its decay over the domain are captured in a finite duration, and decay to zero beyond a finite number of time steps implies a system with zero eigenvalues. We demonstrate propagationsystem identification with pulse response data derived from supercomputer analysis, and conclude that, using superstable-identified systems, we are able to create reusable and reducible propagation-system models that accurately simulate the wave field using a fraction of the original computational resources.

15. SUBJECT TERMS

16. SECURITY CLASSIFICATION OF:			17. LIMITATION OF ABSTRACT	18. NUMBER OF PAGES	19a. NAME OF RESPONSIBLE PERSON
a. REPORT **unclassified**	b. ABSTRACT **unclassified**	c. THIS PAGE **unclassified**		**16**	

Standard Form 298 (Rev. 8-98)
Prescribed by ANSI Std Z39-18

gation from single or multiple sources, in exterior settings with realistic natural terrain, natural media, or man-made features, can be visualized using results of 3D high-performance computing (HPC). Time-domain results typically reveal propagating waves plus reverberations typical of multi-path scattering and wave-guide behavior, with decay toward quiescent motions after the dominant wave energy from duration-limited sources moves out of the domain. Because such computations are expensive and yield data sets with a very large number of outputs, i.e., beyond 10^6 output locations in recent work, it is advantageous to identify a reusable and reducible system for both direct and reciprocal simulations.

Our HPC computations include finite-difference time-domain (FDTD) analyses of linear propagation media. For example, our FDTD computations for propagation within a time-invariant acoustic model solve the following first-order partial differential equations:[1]

$$\frac{\partial P}{\partial t} = -\rho c^2 \left(\frac{\partial v_1}{\partial x_1} + \frac{\partial v_2}{\partial x_2} + \frac{\partial v_3}{\partial x_3} - Q \right)$$

$$\frac{\partial v_1}{\partial t} = -\frac{1}{\rho}\left(\frac{\partial P}{\partial x_1} + \sigma v_1 \right), \qquad \frac{\partial v_2}{\partial t} = -\frac{1}{\rho}\left(\frac{\partial P}{\partial x_2} + \sigma v_2 \right), \qquad \frac{\partial v_3}{\partial t} = -\frac{1}{\rho}\left(\frac{\partial P}{\partial x_3} + \sigma v_3 \right) \tag{1}$$

where $P(x_1, x_2, x_3, t)$ is pressure, our output variable of primary interest; $v(x_1, x_2, x_3, t)$ is the particle velocity vector with components v_1, v_2, and v_3; $\rho(x_1, x_2, x_3)$, $c(x_1, x_2, x_3)$, and $\sigma(x_1, x_2, x_3)$ are the spatially varying material density, speed of sound, and flow resistivity, respectively; and Q is a dilatation-rate source. The method discretizes the solution domain using second-order finite differences both in time and on a Cartesian variable staggered grid. It applies an absorbing boundary condition at the model edges.[2] Leapfrog computations solve the difference equations explicitly, starting from a quiet initial condition. We assign zero flow resistivity to the acoustic propagation media for which we will identify a linear system, and nonzero flow resistivity to model sound absorption by porous ground.

Our objective is efficient simulation of the wave-field response to sources with arbitrary time series. We approach this as a post-processing step for FDTD analyses, by quantifying the decaying pulse response over 2D and 3D sub domains of our numerical linear-time-invariant (LTI) wave-field system. Working with the pulse response is a classical approach, but we wish to make use of state-space mathematics for its computational advantages. This requires identification of a state-space model.

Our initial identification technique applied a variation of the Eigensystem Realization Algorithm (ERA).[3, 4] We followed this process:

(1) By FDTD analysis, generate responses over output wave-field domains using a single input. The input time series can be impulsive with a dominant bandwidth that extends no higher than the accurate frequency range of the FDTD computation. Select the duration to ensure that responses over the output domains decay everywhere to an accepted quiet or still state, i.e., to ensure an acceptable dynamic range.

(2) By Fourier analysis, calculate frequency and pulse responses from input and output time series. Use the pulse response terms as the Markov parameters in the identification problem.

(3) By a modified-ERA analysis,[5,6] identify a state-space model. The model can be used for subsequent wave-field simulations using inputs with the original source location and configuration but with user-definable time series.

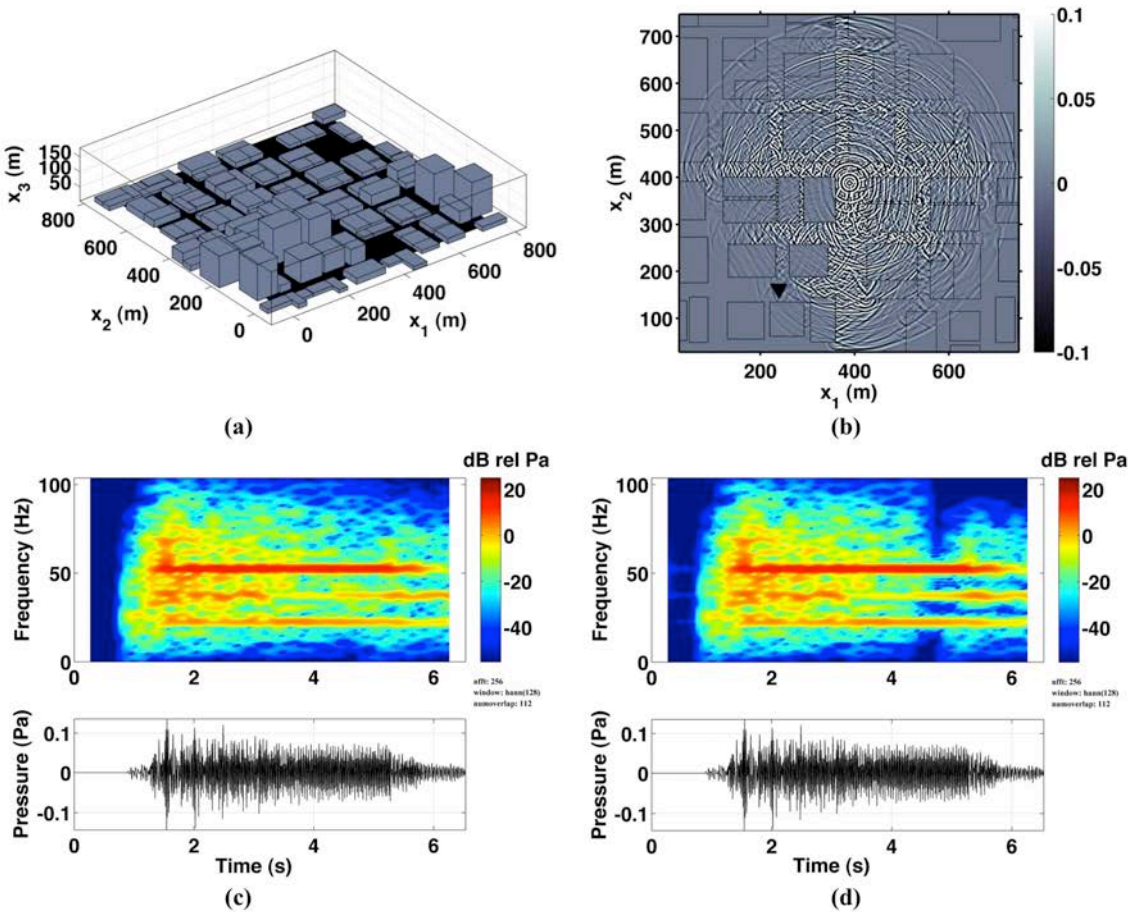

Figure 1. Example result using ERA. (a) Geometry of model for urban acoustic propagation by FDTD analysis. An impulsive sound source at the model center, just above ground, was used to generate Markov parameters. (b) Result from FDTD verification analysis, showing snapshot of pressure field (Pa) above ground and rooftops at time = 1.085 s, from a source containing early pulses and continuing sinusoids. Triangle symbol shows location of extracted signals. (c) Spectragram and extracted signal from FDTD analysis. (d) Corresponding spectragram and signal from simulation using ERA-identified model. The ERA-model simulation produced the illustrated level of fidelity throughout the pressure wave field using a circa 2009 laptop and approximately one millionth of the resources of the HPC analysis, as quantified by (#cores×duration×memory used).

This modified ERA, similar to ERA using data correlations,[7] defines Hankel matrix products containing auto- and cross-correlation sequences of the pulse response. We are specifically interested in simulation-generated systems where the number of outputs is much larger than the number of inputs, and developed the modified ERA to require singular value decomposition (SVD) of a Hankel matrix product whose row and column dimensions depend on the number of time steps in the pulse response, and not on the number of outputs. For our bandwidths and durations the number of time steps is typically in the hundreds, and so the SVD is of a small matrix. The modified ERA successfully creates state-space models with model order equal to the number of time steps of a fully decayed wave-field pulse response, and it supports subsequent model-order reduction.[5,6] Figure 1 highlights an example result.

From our work with ERA, we recognized propagation model features allowing development of what we call a superstable-system identification technique.[8] These features are that the pulse

response over the domain and its decay to a negligible level are, for practical purposes, captured in a finite duration; that decay to zero beyond a finite number of time steps implies a system with zero eigenvalues; and that physical modal frequencies and damping ratios are not applicable. A resulting superstable model has the form of a state-space model but the output matrix contains the pulse response, i.e., the output matrix contains the finite-time system dynamics. The system matrix contains zeros and a sub diagonal of ones. The system order equals the number of time steps. With these features the identification is direct, the system is stable, and simulations have the fidelity of the pulse response. Here we show that a superstable model derived from an HPC-generated wave-field response is particularly suited to large-domain wave-propagation simulations. Our example is an FDTD infrasonic propagation model.

SUPERSTABLE REPRESENTATION

In this section we review the derivation of the superstable state-space representation,[8] and highlight features that allow direct system realization from finite-duration large-wave-field pulse responses. State-space equations for a discrete LTI system (A, B, C) are:

$$x(k+1) = Ax(k) + Bu(k), \qquad y(k) = Cx(k) \tag{2}$$

where x is an n-dimensional state vector; u is an r-dimensional input vector; and y is a q-dimensional output vector. A is the $n \times n$ system matrix, B the $n \times r$ input matrix, and C the $q \times n$ output matrix. k is the time index. The Markov parameters h_k, each with dimension $q \times r$, characterize the pulse response of this system as

$$h_1 = CB, \; h_2 = CAB, \; h_3 = CA^2B, ..., \; h_k = CA^{k-1}B, \quad k = 1, 2, ..., p. \tag{3}$$

The realization problem is stated as follows: given a sequence of $q \times \mathrm{r}$ Markov parameters, find a state-space model (A, B, C) such that Equation (2) holds and the state-space dimension is minimal.[4,9] A minimum realization has the same input-output behavior to some degree of accuracy.[4]

Derivation

To derive the superstable representation, we start with the auto-regressive moving-average model with exogenous input (i.e., ARX). This input-output model has the (order-p) form

$$\begin{aligned} y(k) = \alpha_1 y(k-1) + \alpha_2 y(k-2) + ... + \alpha_p y(k-p) + \\ \beta_1 u(k-1) + \beta_2 u(k-2) + ... + \beta_p u(k-p), \end{aligned} \tag{4}$$

which can be put into state-space form using

$$\tilde{A} = \begin{bmatrix} \alpha_1 & I & 0 & 0 & 0 \\ \alpha_2 & 0 & I & \ddots & \vdots \\ \alpha_3 & 0 & 0 & \ddots & 0 \\ \vdots & \vdots & \vdots & & I \\ \alpha_p & 0 & 0 & \cdots & 0 \end{bmatrix}, \quad \tilde{B} = \begin{bmatrix} \beta_1 \\ \beta_2 \\ \beta_3 \\ \vdots \\ \beta_p \end{bmatrix}, \quad \tilde{C} = \begin{bmatrix} I & 0 & 0 & \cdots & 0 \end{bmatrix}. \tag{5}$$

where $(\tilde{A}, \tilde{B}, \tilde{C})$ is the observable canonical form.

With the Markov parameters in Equation (3), the unit pulse response involving the p Markov parameters, starting from zero initial condition, has the form

$$y(k) = h_1 u(k-1) + h_2 u(k-2) + ... + h_p u(k-p). \tag{6}$$

Equation (6) is the finite impulse response model. If we view Equation (6) as a special case of the ARX model Equation (4), then the corresponding version of Equation (5) is

$$\bar{A}_1 = \begin{bmatrix} 0 & I & 0 & 0 & 0 \\ 0 & 0 & I & \ddots & \vdots \\ 0 & 0 & 0 & \ddots & 0 \\ \vdots & \vdots & \vdots & & I \\ 0 & 0 & 0 & \cdots & 0 \end{bmatrix}, \quad \bar{B}_1 = \begin{bmatrix} h_1 \\ h_2 \\ h_3 \\ \vdots \\ h_p \end{bmatrix}, \quad \bar{C}_1 = \begin{bmatrix} I & 0 & 0 & \cdots & 0 \end{bmatrix}. \tag{7}$$

Direct substitution reveals that $(\bar{A}_1, \bar{B}_1, \bar{C}_1)$ in Equation (7) reproduces the p Markov parameters in Equation (3). The I and 0 matrices in Equation (7) are of dimensions $q \times q$, where q is the number of outputs. The state-space model Equation (7) has q outputs, r inputs, and pq states. For a system with a small number of inputs and a large number of outputs, the dimension of this model is large.

Our interest is a minimal system for the large output problem, and so we will work with the transposed Markov parameters instead of the original Markov parameters. These are

$$h_k^T = \left(CA^{k-1}B\right)^T = B^T \left(A^T\right)^{k-1} C^T = C^* \left(A^*\right)^{k-1} B^*, \quad k = 1, 2, ..., p. \tag{8}$$

where $C^* = B^T$, $A^* = A^T$, and $B^* = C^T$. The Markov parameters of the starred system (A^*, B^*, C^*) are the transposes of the Markov parameters of the original system (A, B, C). Following the approach above leading to Equation (7), a valid state-space realization of the (A^*, B^*, C^*) system is

$$\bar{A}_2^* = \begin{bmatrix} 0 & I & 0 & 0 & 0 \\ 0 & 0 & I & \ddots & \vdots \\ 0 & 0 & 0 & \ddots & 0 \\ \vdots & \vdots & \vdots & & I \\ 0 & 0 & 0 & \cdots & 0 \end{bmatrix}, \quad \bar{B}_2^* = \begin{bmatrix} h_1^* \\ h_2^* \\ h_3^* \\ \vdots \\ h_p^* \end{bmatrix}, \quad \bar{C}_2^* = \begin{bmatrix} I & 0 & 0 & \cdots & 0 \end{bmatrix}. \tag{9}$$

$(\bar{A}_2^*, \bar{B}_2^*, \bar{C}_2^*)$ in Equation (9) is the state-space model of the transposed system (A^*, B^*, C^*), not the original system. We convert $(\bar{A}_2^*, \bar{B}_2^*, \bar{C}_2^*)$ back to the original system. In so doing, we arrive at the following superstable realization for the original system:

$$\bar{A}_2 = \begin{bmatrix} 0 & 0 & 0 & \cdots & 0 \\ I & 0 & 0 & \ddots & \vdots \\ 0 & I & 0 & \ddots & 0 \\ \vdots & \vdots & \vdots & & 0 \\ 0 & 0 & \cdots & I & 0 \end{bmatrix}, \quad \bar{B}_2 = \begin{bmatrix} I \\ 0 \\ 0 \\ \vdots \\ 0 \end{bmatrix}, \quad \bar{C}_2 = \begin{bmatrix} h_1 & h_2 & h_3 & \cdots & h_p \end{bmatrix}. \tag{10}$$

The superstable model $\left(\bar{A}_2, \bar{B}_2, \bar{C}_2\right)$ has q outputs, r inputs, and p states.

Features and Significance

A superstable model is a finite-time state-space model equivalent to the finite impulse response (FIR) model. Direct substitution reveals that Equation (10) reproduces exactly the p Markov parameters in Equation (3). In applications of system response during a specific duration of interest, this representation is sufficient. The transient dynamics of the system need not vanish during this period for the model to be applicable. Although the representation is fundamentally finite-time, the model may still be used to predict beyond the desired duration if the dynamics of the system is such that its transient response is negligible at the end of the finite time duration of interest, which is our routine practice.

Interestingly the superstable system matrix contains no dynamics. The system matrix has zero eigenvalues regardless of the dynamics of the system that it models. The zero eigenvalues cause the Markov parameters to vanish identically beyond a finite number of time steps. The resulting stable model behavior gives the technique its name. In a typical state-space model, the system characteristic information (frequencies, damping ratios) is present in the system matrix, which governs the transient response of the model. The concepts of modal identification are not applicable to wave propagation where large dimensions preclude standing waves. This makes the superstable model ideally suited to external wave propagation, since while the waves may echo and become trapped temporarily, for example by terrain features or structures, they always dissipate.

As explained in the Introduction we select our FDTD model duration to have negligible Markov parameters beyond this duration. It is a design choice to assign this cutoff, and the true FDTD response would attenuate toward floating-point precision. This is analogous to a decaying vibration measurement. Our practice is to impose an ending taper that imposes exactly a zero condition at the end of the FDTD response, and consider this pulse response our truth model. In the case of a source with excitation beyond the duration of the Markov parameters, the model will produce a response with accuracy reflecting the design dynamic range. However, if we consider the FDTD computation with attenuation toward numerical precision to be the truth model, then we recognize that the realization is exact only up to the last Markov parameter h_p and not beyond because the additional Markov parameters formed from Equation (10) are identically zero. This will render Equation (10) invalid beyond the p-time-step duration, which highlights the importance of selecting the duration to ensure that the Markov parameters of the numerical system are negligible from that point on.

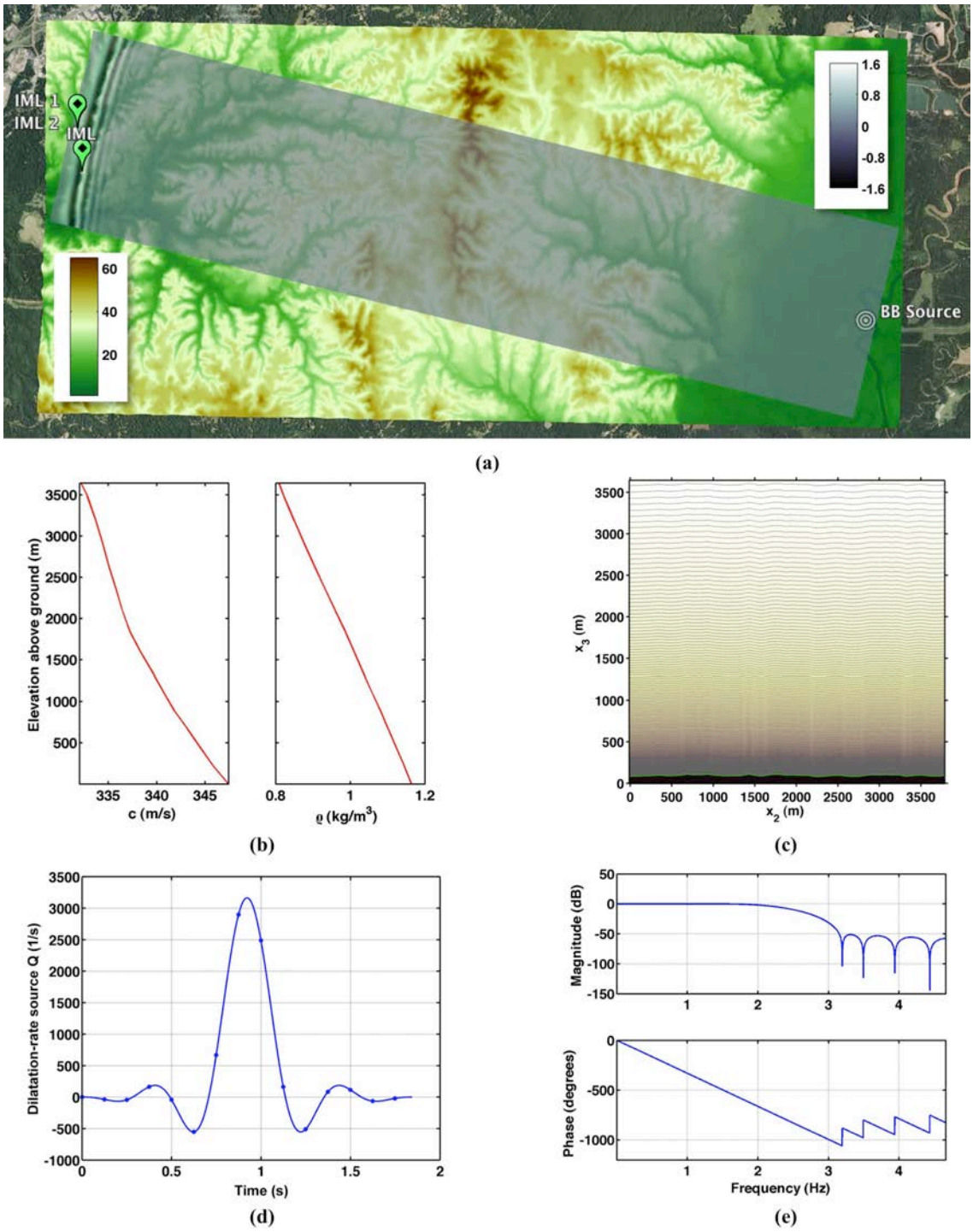

Figure 2. FDTD computation of superstable model. (a) Areal view of setting (North at top) showing source location, sensor locations, and topography and partially transparent snapshot overlays from FDTD output. Snapshot shows waves from impulsive source passing sensors at 42.8 s simulation time. Insets show color scales for topography (lower left) in meters, and pressure (upper right) in Pascals. (b) Profiles of wave speed and density. (c) Illustration of discrete layers used to approximate material profiles. (d) Source history. (e) Frequency response of filter used to generate source.

In our wave propagation problems, the number of outputs q is in the hundreds of thousands or millions whereas the number of inputs r is 1 for a single source, thus a huge reduction in dimensions is achieved. The significance is that a time-consuming realization can now be bypassed. Given the wave-field Markov parameters, in our case via Fourier analysis to calculate the pulse response, a minimum superstable model of the system can be immediately obtained without any further computation. There is no limitation in representing any propagation or other physical phenomenon as long as it is linear and the time duration of interest produces reasonable dimensions for computations, although state-space based model reduction techniques can be applied to reduce the dimension of the model further if warranted.

INFRASONIC PROPAGATION MODEL

Infrasound is sound below 20 Hz. It can propagate very long distances and remain at measurable levels. At local ranges, e.g., on the order of 10 kilometers, terrain relief is capable of scattering and blocking the propagation. This is because the infrasound wavelengths are near the scales of topographic features. These interactions have been observed and quantified by experimental data and models.[10] Our model, which we created for FDTD analyses of Equations (1), is summarized by Figure 2. It spans nearly 15 km to simulate propagation between an impulsive just-above-ground source at the U.S. Army Engineer Research and Development Center (ERDC) Big Black Test Site (BBTS) and an infrasound-sensing array at the ERDC Waterways Experiment Station (WES). Both are in Mississippi. Topographic relief between these locations is just under 70 m. Figure 2 (a) shows the areal extent of the model, whose grid is a rectangular box in three dimensions with a height of 3633 m. The grid aligns with S 77.5^o E, which is the direction between the center of the WES array labeled "IML 1" (IML refers to the locations of Inter-Mountain Labs sensors) and source location labeled as "BB Source." Stretching is applied so that the grid has higher resolution at the ground surface and adjacent to the source and sensor locations. The minimum grid spacing is 2.75 m horizontally and 2.44 m vertically. The grid contains over 325 M nodes.

The model assigns material properties at the appropriate locations to represent topographic relief and atmospheric profiles. The topography is a stair-cased interface between ground and air derived from digital elevation data.* Ground properties model porous sand; these are flow resistivity $\sigma = 5\times10^4$ Pa-s/m^2, effective density $\rho = 11.7$ kg/m^3, and effective wave speed $c = 151$ m/s. The model uses air-layer properties based on gridded weather forecast data.† Our interest is forecast data for 18:47 UTC on September 9, 2011, which is the time of a 10.9-kg C-4 explosive blast at the BBTS. Figure 2 (b) illustrates the atmospheric conditions and wave speed and density profiles estimated for these conditions. The model includes just over 200 air layers, as illustrated in Figure 2 (c), with layer thickness increasing with elevation, to approximate the sound speed and density profiles. We are interested in numerical accuracy associated with 10 nodes per wavelength. The fully stretched node spacing and the minimum wave speed in the profile results in a 3-Hz-accurate bandwidth for the grid. This is high enough for comparison with available field data from the blast source.

* http://nationalmap.gov
† http://nomads.ncdc.noaa.gov

Calibration Analysis to Generate Markov Parameters

The first FDTD analysis was to generate response data for calculating Markov parameters of selected output domains. The analysis applied an impulsive dilatation-rate source at coordinates within the model corresponding to the BBTS blast source location, 1.2 m above the ground surface. We assigned to the source an arbitrary amplitude (3160 $m^3/m^3/s$ peak) with a time series to ensure that the frequency content of the source energy was effectively contained within the 3-Hz model bandwidth. Figure 2 (d-e) illustrate the source time series and frequency content. Our theory and computations are for linear response, and thus our source approximates an equivalent-linear explosive impulse.

The FDTD analysis ran with a 0.000225-s sampling interval and produced 512 output time steps with a 0.1249-s sampling interval (4.004-Hz Nyquist frequency), reaching a level with acceptable decay for generating Markov parameters. It used 256 cores for 12 h 45 min on a Cray XE6.* The cores were within 16 computational nodes, with each node having 32 GB of memory. The output domain presented here is a parallel-to-topography slice with 456×1544-output locations, approximately 3 m above the ground. At this level the effect of terrain relief on the propagation is evident, as indicated by the topography-imaging character of Figure 3 and subsequent overlay results.

Figure 3. Areal view with overlay showing pressure level from FDTD output to impulsive source of Figure 2 (d). Level is for sum-of-squares of signals at each model location. Color scale (lower left) is in dB relative to 1 Pa. Second overlay, evident around the source location, shows pressure level of corresponding superstable model in dB relative to the FDTD value—i.e., the difference in dB levels between the superstable and FDTD integrated signals. This overlay is set to be transparent below ±0.005 dB, an arbitrary threshold that is approximately 0.06 percent relative error. It saturates the color scale at ±0.05 dB.

Figure 3 presents a measure of pressure level throughout the aboveground domain from the FDTD simulation. From the pulse response data underlying the image in Figure 3, we created a 512-state superstable model by populating the C Matrix of Equation (10). As expected, the fidel-

* http://www.erdc.hpc.mil/hardware/index.html

ity of the superstable model to the FDTD simulation is high when excited using the calibration source, which was down sampled to the FDTD-output sampling interval (i.e., the discrete signal outlined by the asterisks in Figure 2 (d)). The difference in superstable and FDTD pressure levels, also illustrated in Figure 3, exceeds 0.005 dB only in the vicinity of the source.

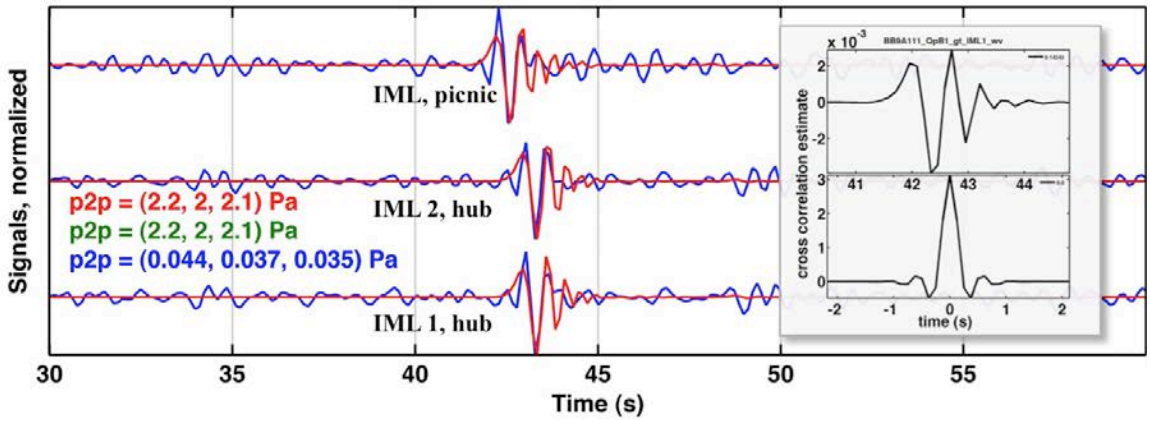

Figure 4. FDTD and superstable model signals from 3 m above the ground compared with measured ground-level data from experimental blast. The lower two signals are from locations corresponding to the nearby IML 1 and 2 sensors, as indicated in Figure 2, and the upper signals are from the location of the IML sensor to the South. The blue lines are the experimental data filtered to a 3-Hz bandwidth. These lines show ambient noise as well as arriving energy from the blast. The red lines are from the superstable model. Green lines, which are hidden exactly below the red lines, are FDTD signals. Peak-to-peak values are listed for each location in order from IML 1. The inset shows a cross correlation result between the source and FDTD IML-1 signals, indicating that the arrival is close to the reported experimental arrival, which was 42.7 s.

With the calibration-model energy levels as background, Figure 4 graphs field signals from the IML locations with corresponding model signals. The IML sensors have a 30-Hz nominal range. We filtered the measured signals with a 3-Hz cutoff and down sampled to a 0.1240-s sampling rate to allow comparison. The model signals show a waveform similar to the field signals at the time of arrival of the source impulse. The peak-to-peak amplitude values given in Figure 4 suggest that a peak dilatation rate close to 20 $m^3/m^3/s$ for the applied source signal in Figure 2 (d) would have produced a good amplitude match. The experimental data shows considerable noise, relative to the source signal, and the source arrival appears to drop below noise levels within about 2.5 s. The model data matches this decay well. The suggestion is that the 3-Hz-bandwidth impulsive-source FDTD model has good fidelity with the experimental data, and thus so do the Markov parameters.

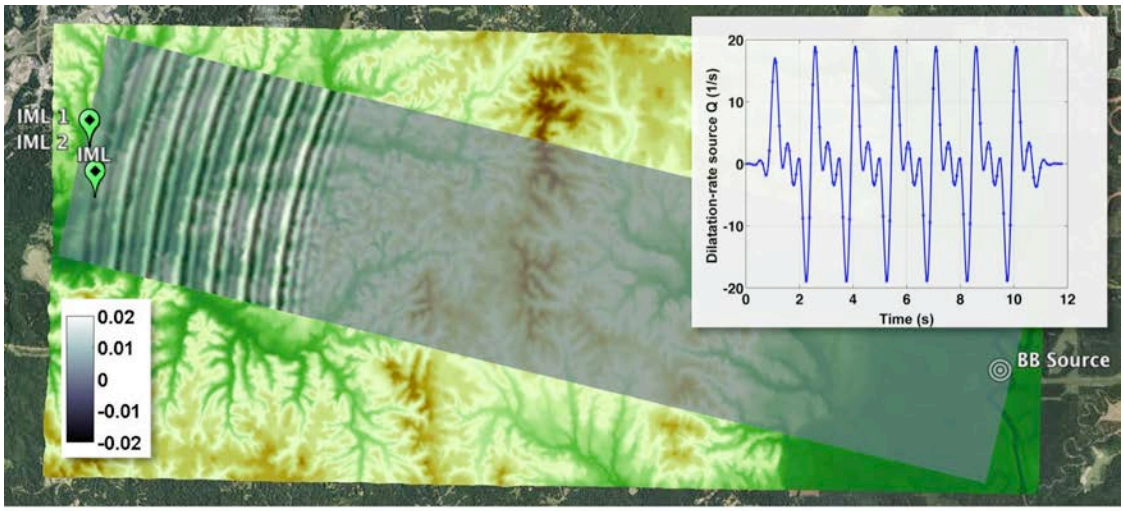

(a)

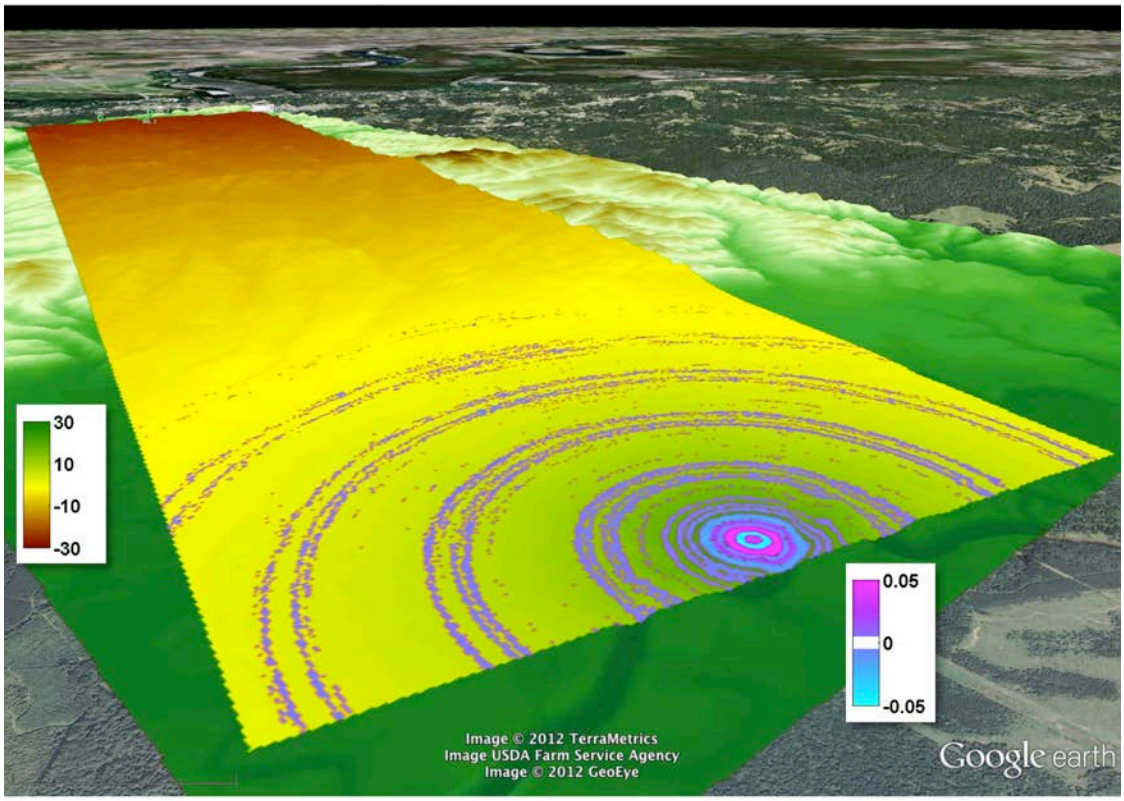

(b)

Figure 5. Results from a sequence of filtered source pulses, generated from superimposed 2/3-, 4/3-, and 6/3-Hz sinusoids over a finite duration. (a) Areal view of FDTD-output snapshot at 42.8 s. Inset shows graph of source history. (b) Oblique view, looking toward the Northwest, with overlay of pressure level from superstable model using down-sampled FDTD source. Level is for sum-of-squares of signals at each model location. Color scale (left) is in dB relative to 1 Pa. Second overlay shows pressure level of the superstable model relative to the FDTD level. It is transparent where below a ±0.005 dB threshold.

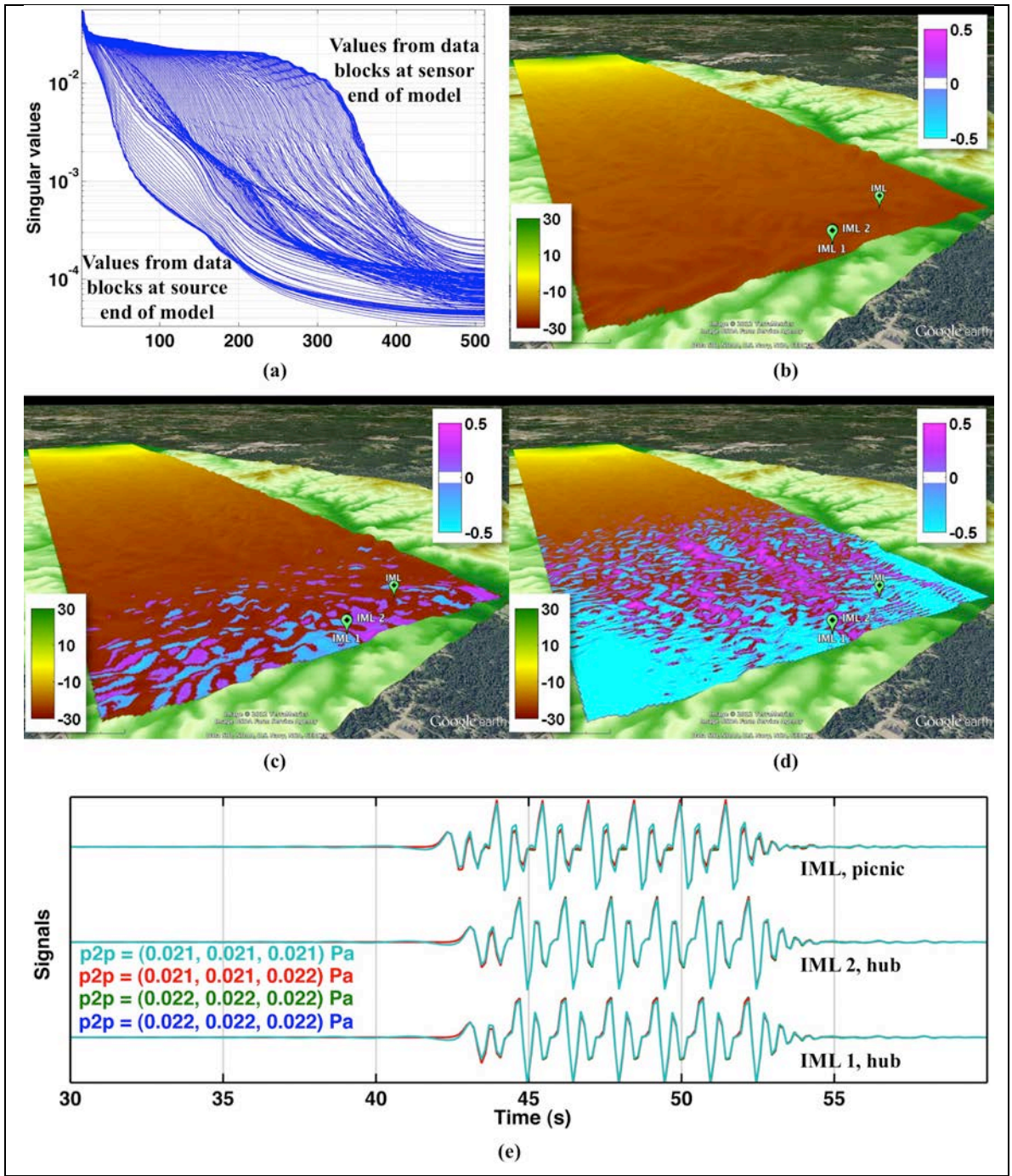

Figure 6. Effect of model-order reduction on results using sequence of finite-duration source pulses. (a) Singular value plots from each of 192 data blocks in output. (b) 512-state superstable model. View toward the Southeast shows overlay of pressure level in dB relative to 1 Pa calculated using sum-of-squares of signals at each model location. Color scale is to the left. Second overlay shows pressure level of the superstable model relative to the FDTD level. Color scale is to the right. Here the transparent threshold is ±0.05 dB, or approximately 0.6% relative error. (c-d) 384- and 320-state reduced-order models, respectively. (e) Signals at the IML locations from FDTD model (blue), 512-state superstable model (green), 384-state reduced model (red), and 320-state reduced model (turquoise).

Verification and Performance of Superstable Model

The second FDTD analysis was to verify that a simulation using the superstable model was accurate for an independent source. The analysis applied a sequence of source pulses, generated from superimposed 10-s-duration 2/3-, 4/3-, and 6/3-Hz equal-amplitude sinusoids, at the location of the source in the calibration model. We filtered the pulses with the response in Figure 2 (e) to ensure the source energy was within the bandwidth of the superstable model. The peak amplitude was nominally 20 $m^3/m^3/s$. Figure 5 illustrates the source time series, a snapshot of the propagation, and the wave-field pressure-level response superimposed on the topography with elevation exaggerated 3× for viewing. This FDTD analysis also processed 512 output time steps with a 0.1249-s sampling interval and used nearly the same computational duration on 256 cores of the Cray XE6 as the calibration analysis, i.e., 12 h 45 min.

Figure 5 (b) illustrates the fidelity of a corresponding 512-step superstable simulation using this second source. The pressure level relative to the FDTD simulation exceeds 0.005 dB in rings surrounding the source, and 0.05 dB in the immediate vicinity of the source, which are very small differences in a practical context. The superstable state-update and output time-series calculations with save-to-file operations lasted 170 s. These used MATLAB®-coded software on a 2.66 GHz Apple MacBook Pro 5,3. The software accessed data using memory-mapping capabilities to avoid reading the Equation-(10) C-matrix data into memory. This data resided in a single-precision 1.44-GB file on an external drive connected by an 800 Mb/sec serial interface. The C-matrix comprised 512-step time series of 704064 outputs. Considering number of cores, average memory per core, and analysis duration, the superstable simulation used approximately one millionth of the computation resources of the FDTD model. While this comparison is for an output that is only about 0.2 percent of the FDTD computational nodes, the savings clearly shows the efficiency in reuse of pre-selected wave-field results by designing the HPC analysis as a superstable-model pre-processing step.

Reduced-Order Models vs. Numerical Prediction

Our superstable state-space dynamic calculations are a streamlined version of the Equation-(2) update equations by virtue of the simple forms of matrices A and B in Equation 10. The states update from the source amplitudes in a loop over the time steps, and the output is the Markov parameter time series multiplied by the state time series. Using this calculation approach is a matter of preference. In state-space form the model is compatible with available state-space based computational and analysis tools including model reduction, model inverse, and Kalman filtering. These tools are not always available for the unit pulse response model that the superstable model replaces. Here we apply model reduction to the superstable model and illustrate the error that results.

Again using the second FDTD response to the Figure 5 source time series as the standard, the 512-state superstable model was reduced using MATLAB® algorithms for balanced realizations and model reductions, and used in simulations performed with the corresponding down sampled source. Because of memory restrictions on the MacBook Pro, we performed the balancing and model reductions in a series of 192 blocks of data, each with 3667 outputs. (In trial analysis we used as few as 8 blocks of 88008 outputs, but arbitrarily chose the larger number of blocks in these calculations). Figure 6 (a) shows the singular-value plots for these blocks, with the difference between ends of the model indicated. Based on inspection of this graph, we produced models with 384 and 320 states to examine the increasing error.

Figure 6 (b-d) show the overlays of pressure level from the 512-, 384-, and 320-state models, respectively. The view is toward the Southeast to highlight the errors in the reduced-order models

at the far end of the model from the source. Here the difference in pressure levels between the 512-state superstable model and the FDTD result does not rise above a ±0.05 dB threshold, or 0.6 percent relative error. In contrast, both the 384- and 320-state models show errors that pass this threshold, with the latter encompassing considerable area.

This relative error, however, is insignificant when considering the FDTD propagation system and the level of fidelity it has to real signals, for example those in Figure 4. This is underscored by the signals comparison in Figure 6 (e), which shows FDTD model signals and the 512-, 384-, and 320-order state-space model signals from the locations of the IML sensors. A difference is just noticeable with the line thickness used in the graph and the significant digits used in the peak-to-peak amplitude values. (The signals plot in the order listed by the Figure 6 (e) caption, and are very close to one another, so that the turquoise and red lines are all that are visible). The implication is that model-order reduction can serve a useful purpose when stored file size is of importance and the reduced accuracy is acceptable. In the 384- and 320-state reduced-order cases, the stored systems would benefit from a reduced size C-matrix, 75 percent and 62 percent of the original 1.44-GB size, respectively, while requiring slightly more storage for the non-trivial A and B matrices.

CONCLUSION

This paper reviews and demonstrates the discrete-time superstable model. The model was motivated by application of the Eigensystem Realization Algorithm to wave-field systems from HPC analyses. Applications of ERA revealed system features allowing superstable model assignment. Most importantly the pulse response and its decay over the domain are captured in a finite duration, and decay to zero beyond a finite number of time steps implies a system with zero eigenvalues. This makes the superstable model ideally suited to wave propagation where large dimensions preclude standing waves and wave energy always dissipates. The model is most efficient when the number of input sources is small, the number of outputs is very large, and the number of samples associated with the finite-time duration of interest is small. When Markov parameters are computed from HPC-derived input-output data, a superstable model can be assigned immediately without additional computation. While a superstable model is a finite-time state-space model equivalent to the finite impulse response model, in state-space form the model is compatible with a wide variety of advantageous state-space based computational and analysis tools. These tools include dynamic simulation, model reduction, model inverse, and Kalman filtering.

Our work here demonstrated propagation-system identification with pulse response data from an infrasonic propagation analysis in which terrain affects the character of the pressure level throughout the wave field. We showed the high fidelity of a superstable simulation to a field-validated supercomputer analysis of propagation from an impulsive source, and verified its accuracy with a numerical analysis using a different source. The superstable result, performed on a laptop, used approximately one millionth of the computation resources of the supercomputer analysis, showing the benefit of designing an HPC analysis as a superstable-model pre-processing step. Application of balanced realization and model-order reduction algorithms to the superstable model demonstrated the advantage of preparing a model in state-space form when accuracy is acceptable and reduced-size file storage is required. We conclude that, by superstable-model identification, we are able to create a reusable and reducible state-space propagation-system model for a given source configuration that accurately simulates large-wave-field time-domain propagation using a fraction of the original computational resources.

ACKNOWLEDGMENTS

This study was in support of the "Denied Area Monitoring Using Infrasound" project performed for the Center Directed Research Initiative at the U.S. Army Engineer Research and Development Center. Computational support was from the U.S. Department of Defense High Performance Computing Modernization Program. Support to Thayer School at Dartmouth was from a Small Business Technology Transfer grant by the U.S. Department of the Army.

REFERENCES

[1] H.H. Cudney, S.A. Ketcham, and M.W. Parker, "Verification of Acoustic Propagation Over Natural and Synthetic Terrain." 2007 DoD High Performance Computing Modernization Program Users Group Conference, IEEE Computer Society, pp. 247-251, 2007.

[2] F.H. Drossaert and A. Giannopoulos, "A Nonsplit Complex Frequency-Shifted PML Based on Recursive Integration for FDTD Modeling of Elastic Waves." *Geophysics*, Vol. 72, No. 2, pp. T9-T17, 2007.

[3] J.-N. Juang and R.S. Pappa, "An Eigensystem Realization Algorithm for Modal Parameter Identification and Model Reduction," *Journal of Guidance, Control, and Dynamics*, Vol. 8, No. 5, pp. 620-627, 1985.

[4] J.-N. Juang, *Applied System Identification*, Upper Saddle River, NJ: Prentice Hall, 1994.

[5] S.A. Ketcham, M.Q. Phan, and H.H. Cudney, "Reduced-Order Wave-Propagation Modeling Using the Eigensystem Realization Algorithm," *Modeling, Simulation and Optimization of Complex Processes*, Proceedings of the Fourth International Conference on High Performance Scientific Computing, March 2-6, 2009, Hanoi, Vietnam, Springer-Verlag Berlin Heidelberg, pp. 183-193, 2012.

[6] S.A. Ketcham, M.W. Parker, and M.Q. Phan, "Realization of Linear Wave-Propagation Models from HPC Simulations," HPCMP Users Group Conference, 2009 DoD High Performance Computing Modernization Program Users Group Conference, IEEE Computer Society, pp. 350-357, 2009.

[7] J.-N. Juang, J.E. Cooper, and J.R. Wright, "An Eigensystem Realization Algorithm Using Data Correlations (ERA/DC) for Modal Parameter Identification," *Control Theory and Advanced Technology*, Vol. 4, No. 1, pp. 5-14, 1988.

[8] M.Q. Phan, S.A. Ketcham, R.S. Darling, and H.H. Cudney, "Superstable Models for Short-Duration Large-Domain Wave Propagation," *Modeling, Simulation and Optimization of Complex Processes*, Proceedings of the Fourth International Conference on High Performance Scientific Computing, March 2-6, 2009, Hanoi, Vietnam, Springer-Verlag Berlin Heidelberg, pp. 257-269, 2012.

[9] B.L. Ho and R.E. Kalman, "Effective Construction of Linear State-Variable Models from Input/Output Functions," *Regelungstechnik*, Vol. 14, pp. 545-548, 1966.

[10] M.H. McKenna, R.G. Gibson, B.E. Walker, J. McKenna, N.W. Winslow, and A.S. Kofford, "Topographic Effects on Infrasound Propagation." *J. Acoustical Society of America*, Vol. 131, No. 1, pp. 35-46, 2012.